COMMUNICATION

Check for updates

A sensitivity analysis of a numbered-up photomicroreactor system†

Koen P. L. Kuijpers,[a] Mark A. H. van Dijk,[a] Quentin G. Rumeur,[a] Volker Hessel,[a] Yuanhai Su*[b] and Timothy Noël*[a]

Limitations with regard to the scalability of photochemical reactions can be efficiently overcome by using numbered-up microreactor technology. Here, the robustness of such a numbered-up capillary photomicroreactor system is tested when subjected to potential disturbances, such as channel blockage and light source failure. Channel blockage leads to relatively large changes in both flow distribution and yield. However, we found that the performance can be accurately predicted thus making it possible to adjust the reaction parameters to obtain certain output targets. Light source failure did not lead to large variations in the mass flow distribution, highlighting the importance of the flow distributor section. Since the reaction is photocatalyzed, the impact on the reaction yield was significant in the reactor where the light failure occurred.

1. Introduction

Process safety, process efficiency and environmentally benign technologies gain increasing amounts of attention in both academia and industry. To improve these important process aspects, microreactors have been suggested as enabling technologies providing enhanced transport phenomena (*i.e.* mass, heat and photon).[1,2] With respect to photochemical transformations, the use of visible light can contribute to develop more energy efficient processes. Such processes allow to use cheap light sources, such as compact fluorescent light bulbs (CFL) or light-emitting diodes (LEDs), and can be even carried out with solar irradiation.[3] Moreover, visible light driven photoredox catalysis gained popularity in the pharmaceutical

industry as it allows to access previously elusive reaction pathways and it provides great functional group tolerance due to the mild conditions, *e.g.* room temperature, atmospheric pressure and lower energy irradiation.[4–8] Consequently, visible-light photochemistry provides a greener and safer alternative to conventional reaction pathways.

Microreactors constitute the ideal reactor platform to carry out light stimulated reactions, as these reactors can overcome the light attenuation effect (Bougueur–Lambert–Beer law).[4,9–11] Typically, photon transport occurs only on a sub-mm scale since the energy is rapidly absorbed by the reaction medium. Sub-mm characteristic dimensions in conjunction with excellent mixing can provide a homogeneous irradiated reaction medium. Furthermore, the reaction time and temperature can be easily controlled in a microreactor, allowing to effectively minimize the formation of by-products, which arise from *e.g.* over-irradiation. Microreactors display also excellent mass transport properties making them perfectly suited for heterogeneous gas–liquid reactions.

Besides all these advantages, the throughput of a single microreactor is typically insufficient for industrial scale production.[12] Traditional scale-up approaches comprise an increase of the channel diameter (scale-out).[13] Such an approach is, however, not feasible for photochemical transformations due to the attenuation effect. However, we and others have recently demonstrated that a numbering-up approach can be a powerful strategy to increase the overall throughput of the process whilst keeping all operating conditions constant.[14–19] Numbering-up is an approach in which several microdevices are placed in parallel. When a single pumping system is used (internal numbering up), the flow must be evenly directed over the parallel reactor channels *via* a flow distributor. However, equal flow distribution over the different channels can be challenging, especially for gas–liquid flow.[20–22]

Multiple factors (*e.g.* fabrication errors, clogging, light failure) can cause flow maldistribution.[23] While fabrication errors can be remediated prior to the launch of a production

[a] *Micro Flow Chemistry and Process Technology, Department of Chemical Engineering and Chemistry, Eindhoven University of Technology, Den Dolech 2, 5600 MB Eindhoven, The Netherlands.* E-mail: t.noel@tue.nl; Tel: +31 40 247 3623

[b] *Department of Chemical Engineering, School of Chemistry and Chemical Engineering, Shanghai Jiao Tong University, Shanghai, P.R. China.* E-mail: y.su@sjtu.edu.cn

This journal is © The Royal Society of Chemistry 2017

React. Chem. Eng., 2017, **2**, 109–115 | 109
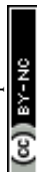
campaign, channel blockage and light source failure deteriorate the performance of the numbered-up system during operation.[24–26] In this work, we carry out a thorough sensitivity analysis with regard to these disturbances. More specifically, we investigate its effect on the overall performance (*i.e.* flow distribution and product yield) of our numbered-up photomicroreactor system.[14]

2. Experimental

2.1 Dimerization of thiophenol *via* photocatalytic aerobic oxidation

Disulfide bonds are widely found in applications ranging from rubber vulcanization agents to pharmaceuticals. We have developed a number of photocatalytic approaches which allow for the mild synthesis of these compounds.[27,28] For this work, we used the photocatalytic oxidation of thiophenol to diphenyl disulfide as a benchmark reaction for the sensitivity analysis (Scheme 1).[27] The reaction utilizes Eosin Y as an inexpensive and metal-free photocatalyst, oxygen gas as the oxidant, *N,N,N′,N′*-tetramethylethane-1,2-diamine (TMEDA) as the base and ethanol as a cheap and green solvent. In flow, this reaction can be completely converted within two minutes while it would take up to 16 hours to complete in batch. This acceleration in flow can be attributed to the optimal gas–liquid mass transfer and the homogeneous irradiation profile. Consequently, such a kinetically fast reaction system is perfectly suited to evaluate the robustness of the numbered-up microreactor system.[14,29]

2.2 Scaled-up multi-capillary photomicroreactor design

The numbered-up capillary photomicroreactor system comprises two main sections, *i.e.* a distributor section and a reactor section (Fig. 1). The entire assembly is solely constructed from commercially available parts and the total assembly time is about one hour, even for non-experts.[29,30] The bifurcated distribution is enabled by the use of T-micromixers (PEEK, 1/16″, 1 mm ID, IDEX Health & Science, Part No. P-714). Consequently, the gas–liquid flow can be split into 2^n streams. In this manuscript, *n* equals 3 resulting in a reactor section with eight parallel capillary microreactors. The transparent microcapillaries are made of high purity perfluoroalkoxy alkane (PFA, 0.75 mm ID, IDEX Health & Science, Part No. 1622L).[31] White light-emitting diode (LED) strips (Paulmann 703.18, 4.8 W, 420 lm, 1.5 m, 12 V) were coiled around the reactor to furnish the required photons. In order to control the temperature (23 °C ± 3 °C), pressurized

air was used to cool the reactors. A schematic representation can be seen in Fig. 1.

Two liquid solutions, the substrate solution and the catalyst solution, are pumped into the system *via* two HPLC pumps (Knauer HPLC pump 1050) and are then combined *via* a T-micromixer to form a single liquid flow. The substrate solution consists of 0.5 M thiophenol in ethanol and α,α,α-trifluorotoluene as an internal standard, while the catalyst solution consists of 1 mol% Eosin Y and 1 equivalent TMEDA as a base in ethanol. The combined liquid flow is merged with an oxygen gas flow, controlled by a mass flow controller (Bronkhorst), resulting in a gas–liquid segmented flow. The segmented flow is then divided into multiple channels *via* the distributor section. After steady state was reached, samples were collected at the outlets of the eight reactors and quenched with a saturated ammonium chloride (NH₄Cl) solution, diluted with ethyl acetate (EtOAc) and analysed with GC-FID (GC-2010 Plus, Shimadzu). The flow distribution was measured by weighing the output of the different reactors over time.

3. Results and discussion

In our previous paper,[14] we already showed that excellent flow distribution could be reached with this setup. Low standard deviation values under reaction conditions ($SD_w < 10\%$) and even lower standard deviations in the absence of any reaction ($SD_w < 5\%$) were obtained. The standard deviation (SD_w) is calculated according to eqn (1) and (2), where w_i is the mass flow rate in a particular reactor channel i, w_m is the average mass flow rate and n is the number of reactor channels in the numbered-up system.

$$SD_w = \sqrt{\frac{1}{n}\sum_{i=1}^{n}\left(\frac{w_i}{w_m}-1\right)^2} \qquad (1)$$

$$w_m = \frac{1}{n}\sum_{i=1}^{n}w_i \qquad (2)$$

3.1 Effect of channel blockage on distribution and yield

Failure of continuous-flow processing can occur because of channel blockage due to solid precipitation.[32,33] Especially for microreactors, clogging remains one of the major hurdles for its widespread implementation.[34] In order to simulate microreactor clogging, we closed off one or multiple channels with plugs. Fig. 2 shows the weight distribution when the first photomicroreactor is blocked. Compared to the situation without channel blockage, all the non-blocked reactor channels experience an increase in throughput. The throughput especially increases in the channel which is paired to the blocked one. This is due to the decreased resistance in this particular section of the bifurcation zone. Interestingly, the
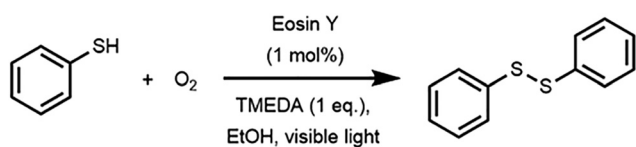
Scheme 1 Dimerization of thiophenol to diphenyl disulfide *via* photocatalytic aerobic oxidation with Eosin Y as photocatalyst.
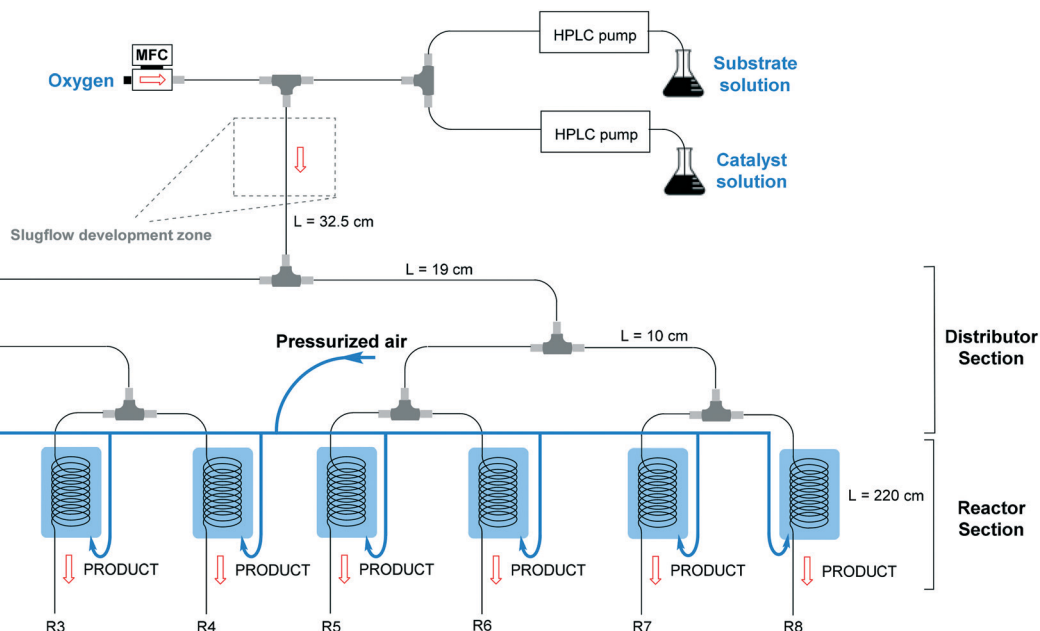
Fig. 1 A schematic overview of the scaled-up reactor system.

other six channels seem to have very similar throughputs within the tested flow range. The standard deviation on the throughput is approximately 15% and therefore slightly higher than the regularly operated set-up where no blockage occurs ($SD_w \leq 10\%$). Our experimental results show the same trend as those reported by Su *et al.*[35,36]

Double channel blockage scenarios are evaluated by respectively blocking reactor 1 and 2, reactor 1 and 3, reactor 1 and 8. For these situations, a higher standard deviation on throughput (SD_w up to 25%) is observed, as can be seen in Fig. 3C. In fact, under such scenarios ($SD_w > 20\%$), the gas-to-liquid ratio, the residence time and the mass transfer between the two phases varies largely and thus affects the overall reaction performance in the numbered-up microreactor system.

Next, we investigated the effect of channel blockage on the yield of the photocatalytic transformation. The average yield of the reaction and its standard deviation are calculated according to eqn (3) and (4), respectively.

$$Y = \sum_{i=1}^{n} \frac{w_i}{w_m} Y_i \tag{3}$$

$$SD_Y = \sqrt{\frac{1}{n} \sum_{i=1}^{n} \left(\frac{Y_i}{Y} - 1 \right)^2} \tag{4}$$

As we have described above, the overall flow rate in the non-blocked channels increases according to the total amount of blockages. This flow rate increase implies that shorter average residence times, and thus lower yields, are obtained (Fig. 3). It is clear from Fig. 3B that when channel blockage occurs the average yield drops compared to the non-clogged situation. For the double blockage scenarios, changes in yield of up to 10% were observed (Fig. 3B).

Theoretically, a decrease in residence time (τ) scalable with the number of blocked channels would be expected, as shown in eqn (5). For instance, when one out of eight channels suffers from blockage, an overall residence time of 7/8 times the original residence time is observed. If the kinetic constant (κ) of the reaction is known and the residence time is indeed scalable in presence of blockage, the expected yield can be calculated. For a reaction with first order kinetics,[29] this yield can be calculated according to eqn (7).

Fig. 2 Weight distribution per total liquid throughput for single blockage.

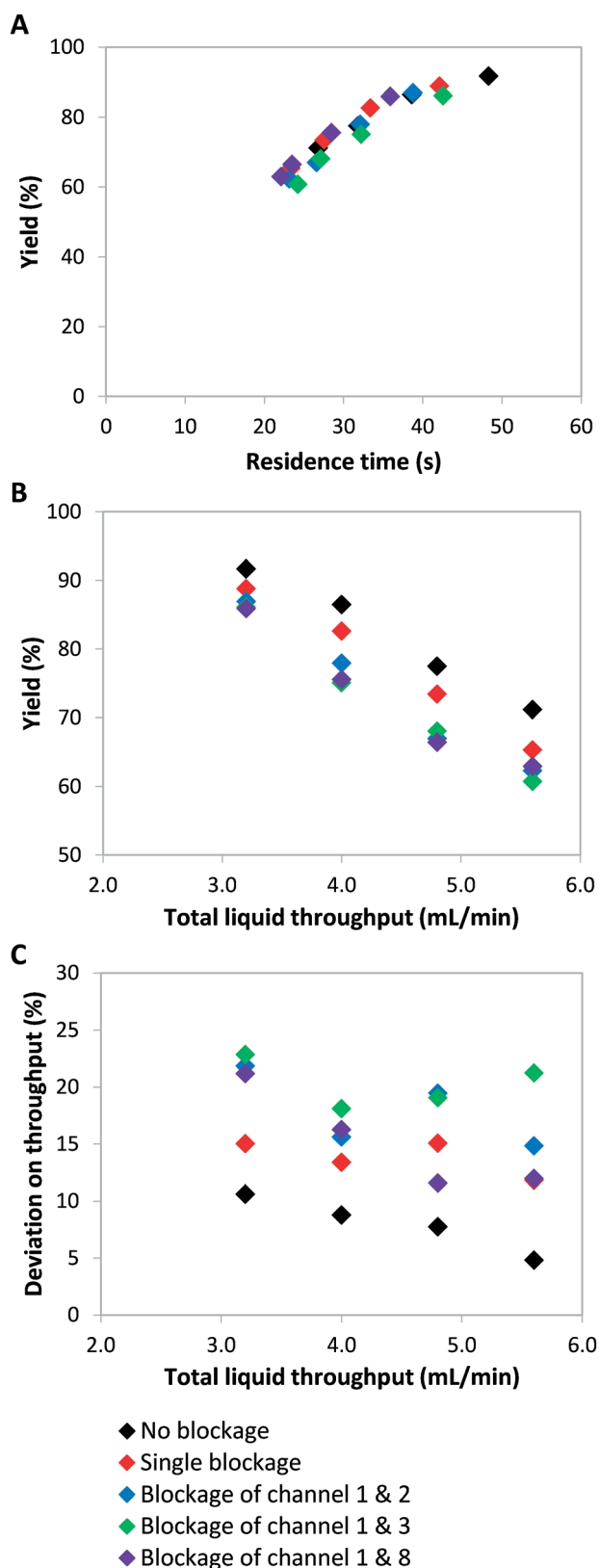$$\tau_{blockage} = \frac{n}{8} \tau_{noblockage} \tag{5}$$

Fig. 3 Reactor performance of the scaled-up system under blocked and non-blocked conditions. A) Reaction yield *versus* residence time. B) Reaction yield *versus* the total liquid throughput. C) Standard deviation on throughput *versus* the total liquid throughput.

Table 1 Confidence intervals for correction factor f_c according to eqn (9)

Case	$f_c \pm \sigma$
Single blockage	1 ± 0.009
Double blockage – channel 1 & 2	1 ± 0.016
Double blockage – channel 1 & 3	1 ± 0.019
Double blockage – channel 1 & 8	1 ± 0.023

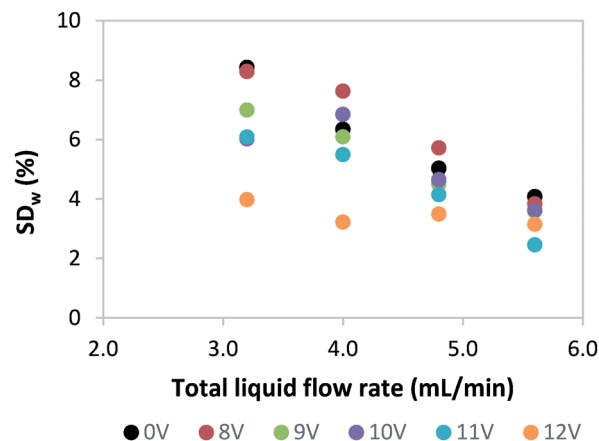**Fig. 4** Weight distribution with variable power in reactor 1.

$$\ln\left(\frac{1}{1-Y}\right) = \kappa\tau \tag{6}$$

$$Y = 1 - e^{-\kappa\tau} \tag{7}$$

$$\frac{Y_b}{Y_{nb}} = \frac{1 - e^{-\kappa\tau_b}}{1 - e^{-\kappa\tau_{nb}}} \tag{8}$$

$$\left(\frac{Y_b}{Y_{nb}}\right)_{experimental} = f_c \left(\frac{Y_b}{Y_{nb}}\right)_{theoretical} \tag{9}$$

The kinetic constant can be determined *via* eqn (6), which represents the integrated standard equation for first order kinetics. This parameter is determined to be $\kappa = 0.0593$ s^{-1} in the numbered-up microreactor in absence of any channel blockage (see ESI†). By applying this kinetic parameter and considering the effect of channel blockage on the residence time (eqn (5)) a comparison between two cases, namely with and without blockage, can be made. This is depicted in eqn (8), where the subscripts nb and b represent the cases of no blockage and blockage, respectively. Obviously, in order to make this comparison the reaction should also obey first order kinetics under blockage. This is checked and can be seen in Fig. 3A, where all data points follow the same first order trend. The theoretical fraction from eqn (8) can then be compared to the experimental results according to eqn (9), where if necessary a correction factor (f_c) can be applied. In the ideal case, this correction factor should be 1. Next, the

112 | *React. Chem. Eng.*, 2017, **2**, 109–115

This journal is © The Royal Society of Chemistry 2017

confidence intervals of f_c are calculated for the four blockage scenarios we tested. The results are shown in Table 1 (more information on the confidence intervals can be found in the ESI†). From these results, it can be understood that the effect of channel blockage on the yield can be very accurately estimated as the standard error in these intervals is rather small. This information should allow the chemical engineer to automatically adjust the flow rates to ensure a given output target. In the meanwhile, the clogged photomicroreactor can be cleaned or replaced. Consequently, the continuous produc-

tion of the target compound is not endangered at any moment during the clogging event.

3.2 Effect of light intensity on flow distribution and yield

Next, we investigated the effect of light source failure on the performance of our numbered-up photomicroreactor assembly. Failure of a light source is a typical issue for a photomicroreactor as a light source can underperform due to aging or can even suffer from total failure. The light source failure
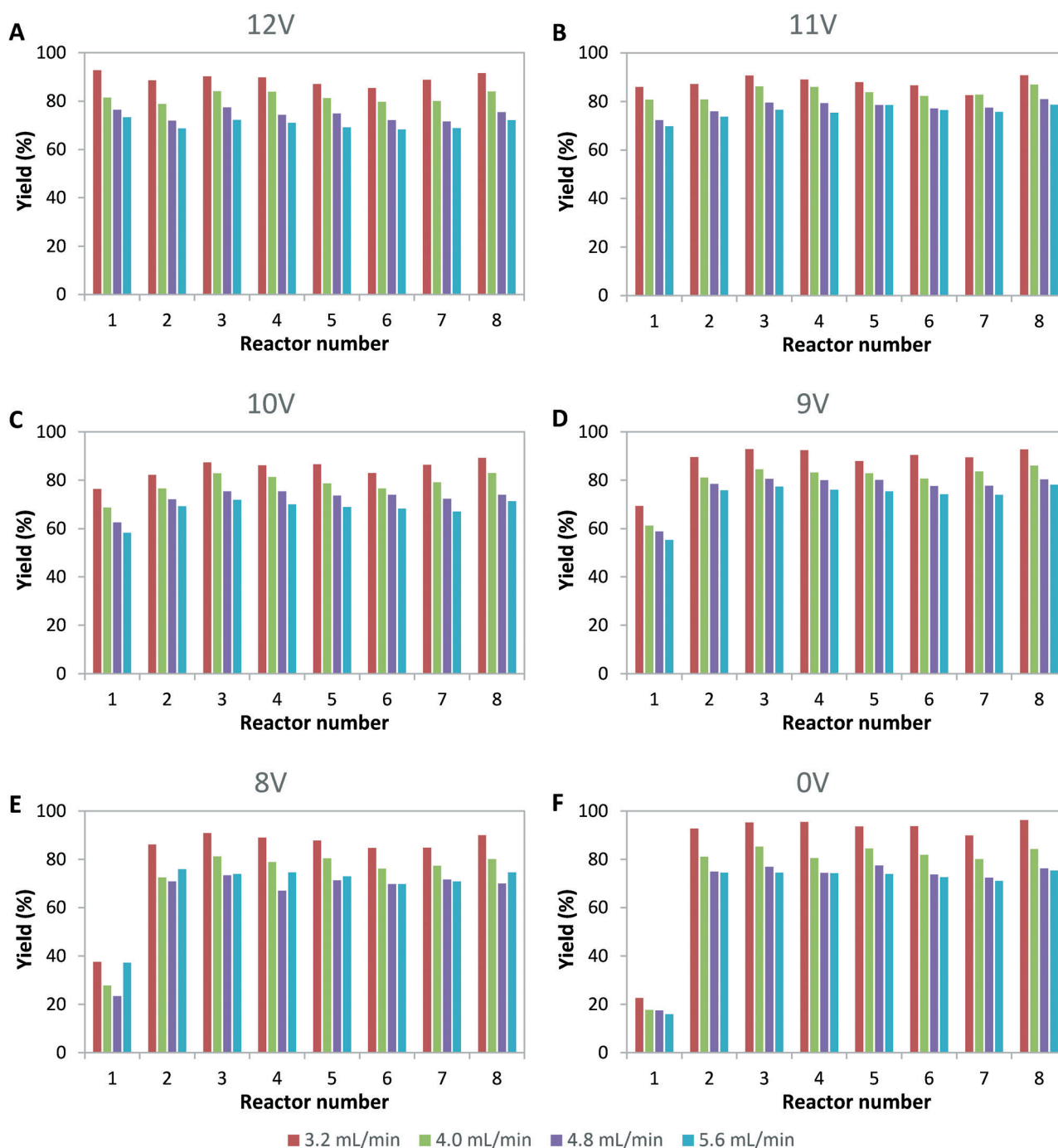

Fig. 5 Yield per channel for variable power input of light for reactor 1 of A) 12 V, B) 11 V, C) 10 V, D) 9 V, E) 8 V and F) 0 V.

This journal is © The Royal Society of Chemistry 2017

React. Chem. Eng., 2017, **2**, 109–115 | 113

can be simulated by decreasing the power input of the LEDs. That is, the power of the light source in one of the reactors is varied over 12 V (standard voltage of the LED strip), 11 V, 10 V, 9 V, 8 V and 0 V. The influence of the variable power on the flow distribution is depicted in Fig. 4. These results demonstrate that the standard deviation is acceptable in all cases ($SD_w < 10\%$). This confirms once more that in such numbered-up systems the distributor section plays the dominant role in the flow partitioning. The ratio of the pressure drop in the distributor section to the pressure drop in the reactor section (see Fig. 1) is the key parameter to obtain proper distribution in gas–liquid flows.[20,29] In order to limit flow maldistribution, this ratio should be between 4 and 25. Our study shows that this principle even holds under light failure disturbances.

Next, we investigated the influence of light failure on the reaction yield in each photomicroreactor (Fig. 5). It can be seen that the reaction yield significantly lowers when the power input of reactor 1 is lowered. This was expected since lower light input results in less photons which are needed to induce the photochemical transformation. Furthermore, the yields of the other seven reactors seem to remain constant. This data shows the robustness of this scaled-up system and its application potential for continuous production.

Conclusions

The flexible scaled-up system used in this research allowed us to measure eight channels individually and therefore an extensive sensitivity analysis based on throughput and yield could be performed. In this study, possible disturbances on a numbered-up photomicroreactor system, like reactor clogging and light source failure, are simulated.

Channel blockage has a significant impact on the flow distribution. The standard deviation on the mass flow rate increased from 10% for no blockage, to 15% for single blockage, up to 25% for the double blockage scenario. Obviously, when one channel is blocked, the flow will be distributed over the remaining reactors. We found that the biggest effect was seen on the paired channel. The overall decrease in residence time, together with the kinetics of the reaction, can be used to estimate the overall yield via a standard yield calculation method. This prediction method was validated and shows high accuracy.

The experiments with variable light intensity show that indeed the reaction is highly sensitive to light irradiation. However, the flow distribution is not affected enormously with standard deviations below 10%. This demonstrates that the flow distributor section is crucial in the design of numbered-up microreactor systems.

We believe that this simple yet effective numbering up system can find its way into academia and industry to enable scale up of flow chemistry. Particularly appealing features of our design are the modularity of the setup, the overall cost of the device, the excellent flow distribution and its stability to flow disturbances.

Notes and references

1 T. Noël, Y. Su and V. Hessel, *Top. Organomet. Chem.*, 2016, **57**, 1–42.
2 R. L. Hartman, J. P. McMullen and K. F. Jensen, *Angew. Chem., Int. Ed.*, 2011, **50**, 7502–7519.
3 D. Cambié, F. Zhao, V. Hessel, M. G. Debije and T. Noël, *Angew. Chem., Int. Ed.*, 2017, **56**, 1050–1054.
4 Y. Su, N. J. W. Straathof, V. Hessel and T. Noël, *Chem. – Eur. J.*, 2014, **20**, 10562–10589.
5 D. Ravelli, S. Protti and M. Fagnoni, *Chem. Rev.*, 2016, **116**, 9850–9913.
6 N. A. Romero and D. A. Nicewicz, *Chem. Rev.*, 2016, **116**, 10075–10166.
7 J. P. Goddard, C. Ollivier and L. Fensterbank, *Acc. Chem. Res.*, 2016, **49**, 1924–1936.
8 D. Staveness, I. Bosque and C. R. Stephenson, *Acc. Chem. Res.*, 2016, **49**, 2295–2306.
9 D. Cambié, C. Bottecchia, N. J. W. Straathof, V. Hessel and T. Noël, *Chem. Rev.*, 2016, **116**, 10276–10341.
10 M. Oelgemoeller, *Chem. Eng. Technol.*, 2012, **35**, 1144–1152.
11 J. P. Knowles, L. D. Elliott and K. I. Booker-Milburn, *Beilstein J. Org. Chem.*, 2012, **8**, 2025–2052.
12 N. Kockmann, M. Gottsponer and D. M. Roberge, *Chem. Eng. J.*, 2011, **167**, 718–726.
13 P. Plouffe, M. Bittel, J. Sieber, D. M. Roberge and A. Macchi, *Chem. Eng. Sci.*, 2016, **143**, 216–225.
14 Y. Su, K. Kuijpers, V. Hessel and T. Noël, *React. Chem. Eng.*, 2016, **1**, 73–81.
15 M. Al-Rawashdeh, F. Yu, T. A. Nijhuis, E. V. Rebrov, V. Hessel and J. C. Schouten, *Chem. Eng. J.*, 2012, **207–208**, 645–655.
16 T. Iwasaki, N. Kawano and J. Yoshida, *Org. Process Res. Dev.*, 2006, **10**, 1126–1131.
17 W. P. Bula, W. Verboom, D. N. Reinhoudt and H. J. Gardeniers, *Lab Chip*, 2007, **7**, 1717–1722.
18 A. Nagaki, K. Hirose, O. Tonomura, S. Taniguchi, T. Taga, S. Hasebe, N. Ishizuka and J. Yoshida, *Org. Process Res. Dev.*, 2016, **20**, 687–691.
19 S. Parisien-Collette, A. C. Hernandez-Perez and S. K. Collins, *Org. Lett.*, 2016, **18**, 4994–4997.
20 M. Al-Rawashdeh, L. J. M. Fluitsma, T. A. Nijhuis, E. V. Rebrov, V. Hessel and J. C. Schouten, *Chem. Eng. J.*, 2012, **181–182**, 549–556.
21 J. Chen, S. Wang and S. Cheng, *Chem. Eng. Sci.*, 2012, **84**, 706–717.

114 | *React. Chem. Eng.*, 2017, **2**, 109–115

This journal is © The Royal Society of Chemistry 2017

22 J. Chen, S. Wang, X. Zhang, H. Ke and X. Li, *Int. J. Heat Mass Transfer*, 2015, **81**, 939–948.

23 C. Amador, A. Gavriilidis and P. Angeli, *Chem. Eng. J.*, 2004, **101**, 379–390.

24 M. Saber, J. M. Commenge and L. Falk, *Chem. Eng. Sci.*, 2010, **65**, 372–379.

25 Y. S. Wada, M. A. Schmidt and K. F. Jensen, *Ind. Eng. Chem. Res.*, 2006, **45**, 8036–8042.

26 P. Pfeifer, A. Wenka, K. Schubert, M. A. Liauw and G. Emig, *AIChE J.*, 2004, **50**, 418–425.

27 A. Talla, B. Driessen, N. J. W. Straathof, L. G. Milroy, L. Brunsveld, V. Hessel and T. Noël, *Adv. Synth. Catal.*, 2015, **357**, 2180–2186.

28 C. Bottecchia, N. Erdmann, P. M. A. Tijssen, L. G. Milroy, L. Brunsveld, V. Hessel and T. Noël, *ChemSusChem*, 2016, **9**, 1781–1785.

29 Y. Su, V. Hessel and T. Noël, *AIChE J.*, 2015, **61**, 2215–2227.

30 Y. Su, A. Talla, V. Hessel and T. Noël, *Chem. Eng. Technol.*, 2015, **38**, 1733–1742.

31 N. J. W. Straathof, Y. Su, V. Hessel and T. Noël, *Nat. Protoc.*, 2016, **11**, 10–21.

32 T. Noël, J. R. Naber, R. L. Hartman, J. P. McMullen, K. F. Jensen and S. L. Buchwald, *Chem. Sci.*, 2011, **2**, 287–290.

33 S. Kuhn, T. Noël, L. Gu, P. L. Heider and K. F. Jensen, *Lab Chip*, 2011, **11**, 2488–2492.

34 R. L. Hartman, *Org. Process Res. Dev.*, 2012, **16**, 870–887.

35 Y. Su, G. Chen and E. Y. Kenig, *Lab Chip*, 2015, **15**, 179–187.

36 Y. Su, A. Lautenschleger, G. Chen and E. Y. Kenig, *Ind. Eng. Chem. Res.*, 2014, **53**, 390–401.

This journal is © The Royal Society of Chemistry 2017

React. Chem. Eng., 2017, **2**, 109–115 | 115